

Investigating the Potential of Hyper-Temporal Terrestrial Laser Point Clouds for Monitoring Deciduous Tree Growth

Anne Bienert*, Katja Richter, Sophia Boehme, Hans-Gerd Maas

Institute of Photogrammetry and Remote Sensing, Dresden University of Technology, Germany – (anne.bienert, katja.richter1, sophia.boehme1, hans-gerd.maas)@tu-dresden.de

Keywords: Hyper-temporal tree recording, growth modelling, forest inventory parameters, terrestrial laser scanning.

Abstract

Monitoring tree growth processes is relevant for ecological research and understanding the intricate relationship between vegetation and the environment. Time series analyses have revealed a correlation between leaf emergence timing and climate change, with earlier leaf emergence attributed to global warming. While traditional forest inventory methods struggle to quantify growth processes on small scales, terrestrial laser scanning provides a powerful alternative for providing high-resolution 3D information. This study explores the use of high-frequency hyper-temporal terrestrial laser scanning data to quantitatively describe deciduous tree growth, tested on a pedunculate oak (*Quercus robur*). The research aims to address key questions about detecting leaf growth in hyper-temporal terrestrial laser scanning data. Additionally, it explores how 3D tree parameters and point cloud comparisons capture leaf and tree growth throughout the year. Results from M3C2 point cloud analyses indicate that the temporary branch movements correlate with precipitation. Over the year, branch movements were detected to increase with growing distance from the trunk.

1. Introduction

The monitoring of tree growth processes is highly relevant for ecological research and for a better understanding of the complex relation between vegetation and environment. Time series studies have shown that the timing of leaf emergence is correlated with climate change and that leaf emergence is occurring earlier due to global warming (Vitasse et al., 2022). Leaf growth in spring and branch growth throughout the year are also important indicators of the effects of climate change on trees and their ability to adapt to changing climatic conditions.

Quantifying growth processes, which take place on small spatial and temporal scales, is difficult using conventional forest inventory methods. Terrestrial laser scanning (TLS) is a powerful alternative, providing high-resolution 3D information on the vegetation structure at almost arbitrary time intervals. The measurement frequency of multi-temporal studies can range from seasonal examinations (Olivier et al., 2017) or daily examinations to hourly examinations (Puttonen et al., 2016; Puttonen et al., 2019; Campos et al., 2021) of vegetation changes. Information on tree growth is usually obtained from 3D tree parameters (e.g. tree height, diameter at breast height (DBH), crown parameters) derived from the TLS point clouds using automated methods (e.g. Maas et al., 2008). Most studies are based on leaf-off data in order to obtain an unobstructed view of the 3D structures in the crown space. In contrast, Hosoi et al. (2011) specifically use leaf-on data to analyze leaf orientation. Dupuis et al. (2017) estimate leaf thickness from point clouds of a two-dimensional laser triangulation sensor combined with a coordinate measuring arm.

This study investigates the potential of hyper-temporal TLS data for monitoring deciduous tree growth. The focus is on two aspects: leaf and tree growth over the course of the year. The subject of the study is a pedunculate oak (*Quercus robur*), which is a central element of forest conversion in the study region due to its adaptability to changing climatic conditions.

With the presented work we want to answer the following research question:

- Is it possible to detect leaf growth in the hyper-temporal TLS data?
- How does leaf growth and tree growth manifest itself in quantitative 3D tree parameters and point cloud comparisons?

When comparing hyper-temporal data, it is important to consider that a tree is not a static object. In addition to growth, one will always see branch movements in the data. Zlinszky et al. (2017) show a nocturnal lowering of the branches, which Juntilla et al. (2022) explain by an increasing water content in the leaves at night.

In addition, the increasing weight of the leaves causes the branches to lower, which manifests itself in an annual cycle. The branch movement is highly correlated to the water status of the plant (Hallmark et al., 2011). Humidity and air temperature, for example, play a major role. Rain also causes the branches to temporarily move. Both phenomena have an effect on the analysis of the hyper-temporal data and must be taken into account when interpreting the results. For this reason, a method for determining branch movements was developed. The basic idea is to track prominent branch points through the entire data set.

2. Data Acquisition

For the study, a hyper-temporal TLS data set of a pedunculate oak (*Quercus robur*) has been recorded. The study site is located in Dresden, Germany (51°1'46" N, 13°43'29" E). The tree is a solitary street tree that does not interact with neighboring trees (Fig. 1). It has a height of approximately 12.2 m and is surrounded by tall buildings. The acquisition of the hyper-temporal TLS data is described in section 2.1. In addition to the TLS data, meteorological data were recorded (Section 2.2).

* Corresponding author

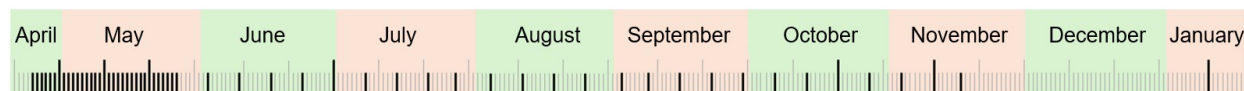


Figure 2. Recording dates.

2.1 TLS Data

TLS data acquisition was carried out during the growing and leaf-on season from April to January. Laser scans were taken daily from the beginning of leaf emergence until the leaves were fully developed, (April 24 – May 26). After that, the measurement cycle was changed to weekly (Fig. 2). The dry leaves remain on the tree well into the winter, and the last leaves do not fall off until January. A final scan was therefore carried out in January. Overall, 60 scan epochs were recorded. The DBH was measured at the beginning and end of the scan epochs using a circumference measuring tape.

The TLS data were acquired with a RIEGL VZ-400i terrestrial laser scanner at a resolution of 40 mdeg from four diametrically arranged positions (Fig. 3). The scanner viewpoints were located approximately 15 m away from the tree at nearly identical positions. For fine registration purposes, 11 retro-reflective targets were attached to the surrounding buildings.

Wind-induced movement of the branches cannot be excluded in natural locations. The effects of wind are amplified by the sequential recording scheme of a laser scanner, which leads to smearing effects in the form of distortions or compression. In this study, a log of the prevailing wind conditions was kept, and the wind direction and strength were measured. The scan was occasionally interrupted during very strong gusts.



Figure 1. Pedunculate oak under leaf-off (April, 2023) and leaf-on (June, 2023) conditions.



Figure 3. Top view of the measurement setup with pedunculate oak (black circle) and the scan positions ScanPos001-ScanPos004.

2.2 Meteorological Data

Meteorological data from a KLIPS weather station (KLIPS, 2024) in the immediate vicinity (<50 m, 51°1'47" N, 13°43' 28.7" E) was available for the measurement period. The sensor node of the weather station faces south and is mounted at a height of 3 meters. Relative humidity and air temperature were recorded at 10-minute intervals. In addition, wind direction and wind speed were measured during scanning using a mobile anemometer right next to the tree.

The daily precipitation amount was extracted from a climate station of the Deutscher Wetterdienst (DWD) Climate Data Center (CDC). The climate station used is about 3.1 km away (51°1'29.64" N, 13°46'30" E).

3. Methods

The hyper-temporal TLS data was first pre-processed (Section 3.1). To analyze leaf growth and tree growth, 3D tree parameters were derived (Section 3.2) and point cloud comparisons were performed (Section 3.3). Additionally, the annual branch movement was analyzed (Section 3.4).

3.1 Preprocessing

The 60 scan epochs were registered with a mean standard deviation of $0.65 \text{ mm} \leq \sigma_0 \leq 1.95 \text{ mm}$ using the retro-reflective targets. Subsequently, the tree was cut out of the entire point cloud in each epoch. For this purpose, a polygon was defined in the XY view of epoch 1 to separate the tree from neighbouring buildings, street signs and street vegetation. The resulting point clouds contain both tree and ground points and are used as input data for deriving 3D tree parameters. Finally, the ground points were removed. The resulting point clouds are used as input data for the point cloud comparisons.

3.2 Determination of 3D Tree Parameters

The parameters tree height, diameter at breast height (DBH), crown projection area (CPA) as well as crown volume were determined for each measurement epoch using the approach presented in Mass et al. (2008) and Bienert et al. (2021) (Section 3.2.1) as well as the commercial software package LiDAR360 (V7.0).

3.2.1 Proprietary method: The method derives the 3D tree parameters fully automatically from the point clouds. The tree height is defined as the difference between the highest and lowest tree point. On sloping terrain, the point on the trunk is on the uphill side. This is also the height basis for the DBH derivation, which is defined as the stem diameter at a height of 1.3 m above a digital terrain model (DTM). To determine the DBH, a section of the point cloud with a height of 10 cm is extracted and a circle fitting is performed.

The crown projection area is obtained by a vertical projection of the tree crown onto the ground. It is determined as a convex hull from the 2D projection of all scan points in the XY plane. The outcome is a set of points representing the surrounding polygon and its corresponding area.

To determine the crown volume, the *polygon method*, employs the extraction of crown projections in equally spaced horizontal layers along the tree crown. The area of the surrounding polygons is multiplied by the layer thickness and subsequently summarized to yield the volume.



Figure 4. Proprietary method for crown volume determination: polygon method with equally spaced surrounding polygons.

3.3 Multiscale Model to Model Comparison

The M3C2 algorithm (Multiscale Model to Model Cloud Comparison, Lague et al., 2013) is a method for analyzing point clouds and to compare two or more point clouds with each other to identify differences in geometry. To compare the point clouds of successive epochs, the M3C2 implemented in CloudCompare was used. In the M3C2 comparison, the surface normals and their 3D orientation are first estimated. Then, the mean area changes along the normal directions are calculated. The registration error is taken into account to assess the significance of the corresponding displacement. Due to the extensive scan epochs, a Python script was developed to initiate the M3C2 plugin via command line mode. Thus, automatic processing was performed using constant M3C2 parameters with scan-specific registration errors. The scan-specific registration errors are calculated based on the average errors of the two scan epochs to be compared.

3.4 Analysis of branch movements

The branch movements are analyzed by tracking natural branch points in the co-registered point clouds of the time series. The workflow (Fig. 5) consists of four steps. The first step involves the interactive identification of discernible branch points p^0 within the point cloud at epoch t_0 . It is preferable that these points exhibit characteristics such as branch forks or distinctive structural features, which will facilitate unambiguous automatic assignment in subsequent stages.

Subsequently, a spatial region N_j^i around each identified branch point is delineated, characterized by coordinate boundaries (X_{min} , X_{max} , Y_{min} , Y_{max} , Z_{min} , Z_{max}). Within each epoch (t_0, \dots, t_n where n denotes the number of epochs), the corresponding point cloud sections are extracted based on these defined boundaries. Notably, the extent of this region is set sufficiently wide (± 20 cm in all spatial dimensions) to allow for a potential displacement of the branches.

The third step entails the application of the Iterative Closest Point algorithm (ICP, Besl and McKay, 1992) on the extracted point cloud sections. This iterative process aims to determine

transformation parameters, with the point cloud data from epoch t_0 serving as reference. Subsequently, the point cloud sections from epochs t_0, \dots, t_n are transformed into the reference system of epoch t_0 .

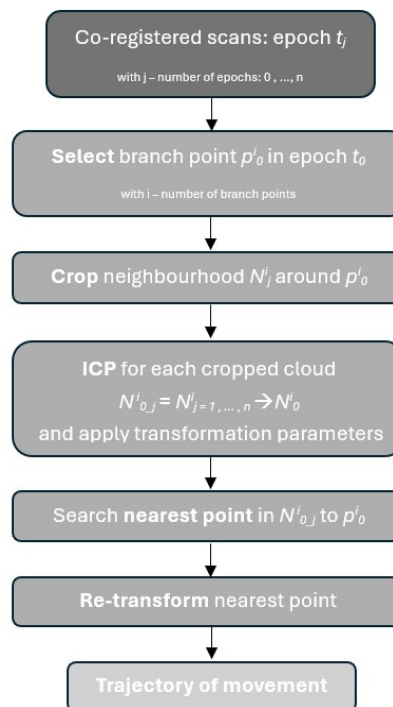


Figure 5. Workflow for tracking branch points in the hyper-temporal TLS data.

After the transformation, the closest point to the original branch point at epoch t_0 is identified via the smallest distance search within the transformed point cloud of the respective epoch. This point will serve as the branch point for the corresponding epoch, which will then be transformed back into the coordinate system of the original epoch. The result of branch tracking is the 3D trajectory of the tracked branch point in all epochs.

To facilitate the process, a Python script was developed to automate the branch point tracking procedure using a predefined list of branch points from epoch t_0 . This script uses the *CROP* and *ICP* routines from CloudCompare (version 2.12.4), invoked in command-line mode.

4. Results and Discussion

This section presents and discusses the results of the meteorological measurements (Section 4.1), the determination of the 3D tree parameters (Section 4.2), the point cloud comparison (Section 4.3) and the analysis of the branch movements (Section 4.4).

4.1 Meteorological Data

Figure 6 illustrates the measured air temperature, relative humidity and daily precipitation height recorded during the scan epochs and averaged over a day. Figures 6a and 6b represent values obtained from a weather station located in close proximity to the scanned tree. The daily precipitation height was recorded by a station in another part of the city. Therefore, it is possible that the actual amount of precipitation for the tree was slightly different.

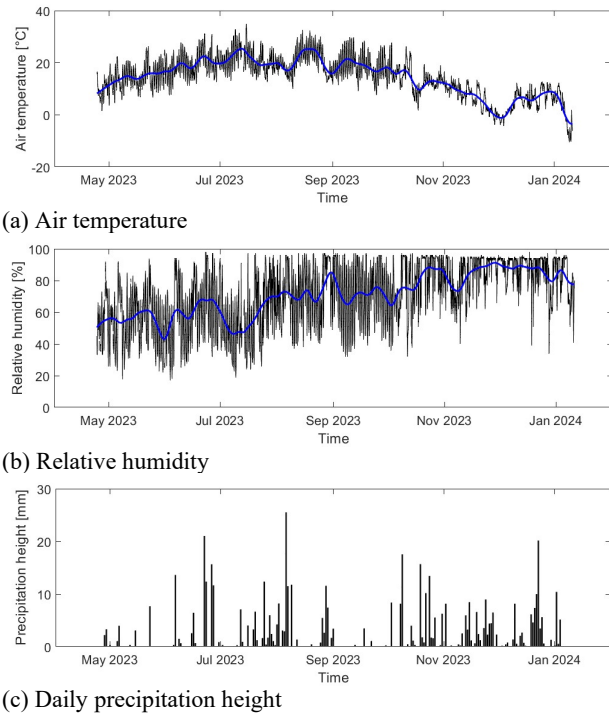


Figure 6. Results of the meteorological measurements: a) Air temperature and b) Relative humidity from a KLIPS-station; c) Daily precipitation height, database: Deutscher Wetterdienst (DWD), Climate Data Center (CDC), single values averaged.

4.2 Determination of 3D Tree Parameters

Tree height: The obtained tree heights (Fig. 7) of both software's show clear differences. Two things stand out in the curve of the tree heights. There is a consistent slight overestimation (4.7 cm) in the commercial software compared to the non-commercial software. Presumably the determination of the tree base is lower when using LiDAR360, which leads to a higher tree height estimate.

Secondly, there is a conspicuous spike evident in both curves around the epochs of May 16 and June 2. The decrease in tree height observed from May 16 to June 2 can be explained by an escalation of ground vegetation. Shortly before June 9, the grass at the location of the tree was mowed, which lead to a lower DTM determination, resulting in a sudden increase in the calculated height of the tree.

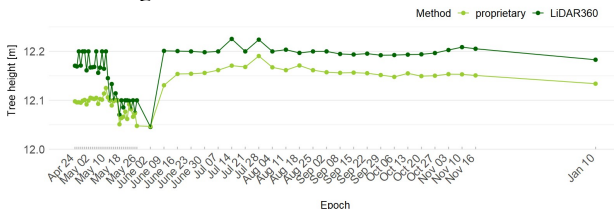


Figure 7. Comparison of the tree height obtained with proprietary method and LiDAR360.

DBH: The DBH demonstrates an increase of approximately 1 cm (Fig. 8). There are slight differences (mean 1.8 mm) in the DBH determination regarding the two methods, which can be caused by different heights on the trunk. If the base of the tree is determined using different methods, the height at the trunk varies by a few centimeters. This discrepancy, along with variations in the thickness of points utilized for circle fitting,

contributes to the observed differences. Different thicknesses of the point cloud sections were used to determine the DBH (10 cm proprietary method vs. 20 cm LiDAR360). Figure 8 shows the DBH obtained and the DBH measured with a circumference measuring tape.

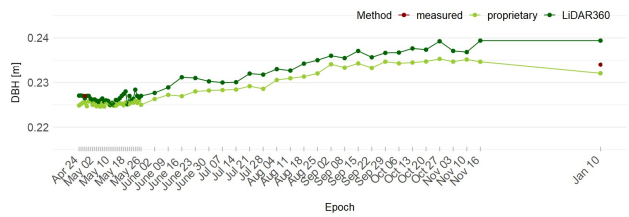


Figure 8. Comparison of the DBH obtained with proprietary method and LiDAR360.

CPA and crown volume: The curves for crown projection area, and crown volume are very similar, characterized by a rapid increase during the leaf growth period followed by relatively constant values throughout the tree growth period (Fig. 9, 10). The CPA values agree well. The last epoch was measured in January, after the leaves had fallen. As expected, the values decrease significantly here.

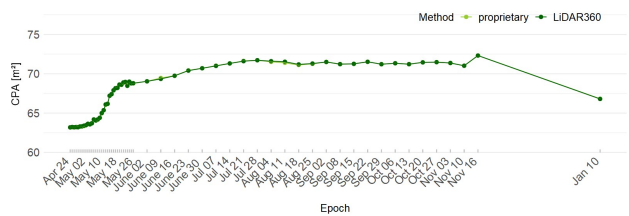


Figure 9. Comparison of the CPA obtained with proprietary method and LiDAR360.

The *polygon method* is used to determine the 3D extension of the crown. However, the actual wood volume is smaller, as the spaces between the branches are taken into account here. The method used by LiDAR360 to determine the volume is not known. It is assumed that the methods determine the volume in different ways and a wide spread of the determined values is therefore expected. However, in order to make it comparable, the results of the polygon method and LiDAR360 are shown in Figure 10.

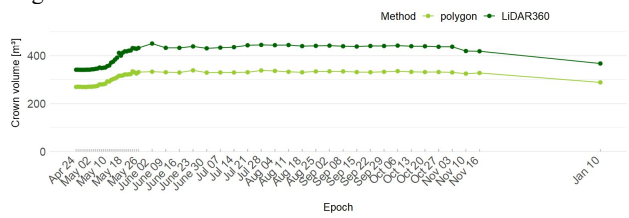


Figure 10. Comparison of the crown volume obtained with *polygon method* and LiDAR360.

The tree height is a parameter that provides good information over a longer observation period for tree growth. The DBH is also an indicator of the growth in wood volume and does not provide any information on leaf emergence. In the rather short time series, the crown parameters show the change in volume as a result of leaf emergence much better.

4.3 Multiscale Model to Model Comparison

The M3C2 comparison was used to visualize vegetation changes in subsequent epochs. The actual leaf emergence started on May 2. Figure 11 shows the results of the M3C2 comparison,



Figure 11. M3C2 distances of two successive epochs with drop-coded precipitation height. During the daily recording, one filled drop represents a precipitation of 1.25 mm and during the weekly recording, one drop symbolizes a precipitation of 11 mm.

where each epoch t_n is shown compared to the previous epoch t_{n-1} . The daily amount of precipitation that fell between the two recording times is visualized as colored drops. From the weekly scans onwards (from May 26), the amount of precipitation per 7 days was indicated. Positive M3C2 distances (vegetation changes as a result of growth) are shown in red and negative distances in blue. Since May 7, a sudden and continuous change in the M3C2 distances can be seen.

Considering the daily scan comparisons (until to May 26), two days stand out on which the M3C2 comparisons show completely opposite results to the subsequent comparison: May 5 - May 6 and May 22 - May 23. When comparing the later epochs, there are differences of up to 12 cm. Interestingly, these anomalies are always observed on days with heavy rainfall. The differences are mostly positive.

From the weekly recording onwards, the distances are rather mixed and irregularly distributed over the recording period. No uniform trend can be seen, possibly due to the warm and rainy weather. From September 22, the M3C2 distances are mostly negative, which can be explained by the beginning of leaf fall.

4.4 Analysis of branch movements

Branch points were randomly distributed in the crown (variation in height and distance from the trunk) at a junction of two branches to analyze the movement as a function of the height and distance of the trunk. The order of branching from the trunk was recorded for each point. With increasing distance of the branch points from the trunk, an increase in branch movement in the Z direction was observed (Figure 12). No correlation could be found between branch movement and the height of a branch within the crown.

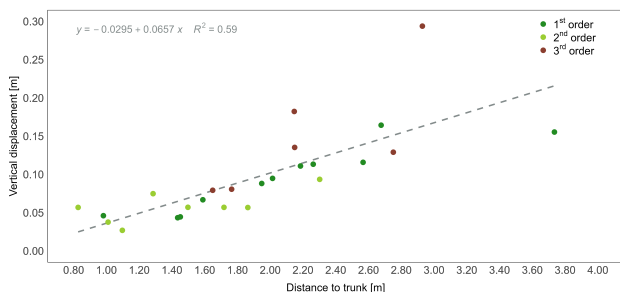


Figure 12. Movement of the branch points in the Z direction as a function of the horizontal distance of the branch points from the trunk. The colors symbolize the order of the branches.

There is not only a movement in the Z direction, but also a movement in the X and Y directions. Figure 13 presents the movement of 8 branch points in the XY, XZ and YZ projections. Concerning the branch points K and O, these are a 2nd order branch point and a 1st order branch point with a height of 7.17 m and a distance of 1.28 m to the trunk, and a height of 6.57 m and a distance of 2.58 m, respectively. Over the course of the year, their movement corresponds roughly to a circular movement. Point M, however, shows an irregularly scattered course in the projections. The attributes of the selected branch points depicted in Figure 13 are described in Table 1.

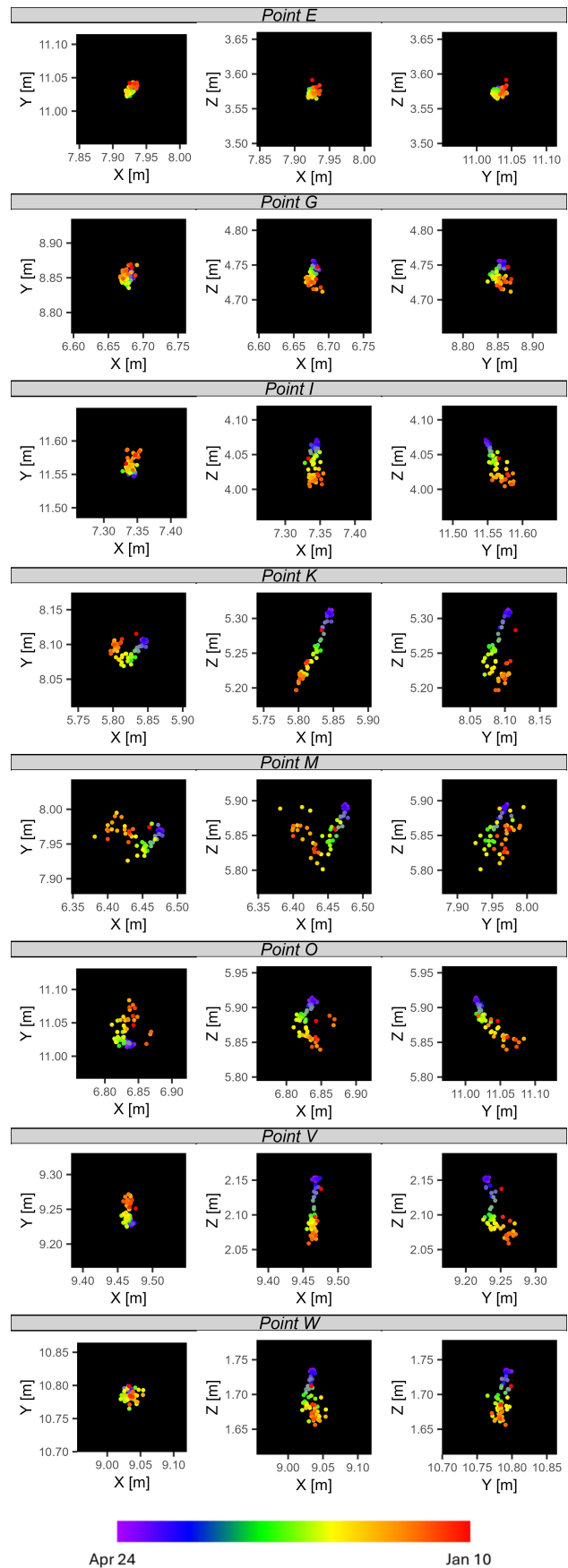


Figure 13. Movement of 8 distinctive branch points in XY, XZ and YZ projection.

Table 1. Characteristics of the selected branch points with branch order Br. ord., height h and distance d_{trunk} of the point to the trunk and the maximum scattering in the coordinate directions ΔX , ΔY , ΔZ . The largest deviations are highlighted.

	Br. ord.	h [m]	d_{trunk} [m]	ΔX [m]	ΔY [m]	ΔZ [m]
E	2	4.84	1.10	0.02	0.02	0.03
G	1	6.01	1.45	0.02	0.03	0.04
I	1	5.33	1.59	0.05	0.05	0.12
K	2	7.17	1.28	0.03	0.04	0.07
M	2	7.15	2.30	0.10	0.07	0.09
O	1	6.57	2.58	0.06	0.07	0.07
V	1	3.41	2.01	0.03	0.03	0.08
W	3	3.00	1.65	0.02	0.05	0.09

The three-dimensional movement over the year for two selected branch points (K and O) is shown in Figure 14. It can be seen that, in addition to the lowering of the branch, a lateral movement of the branch occurs. After leaf fall, the branch returns to the vicinity of the starting point.

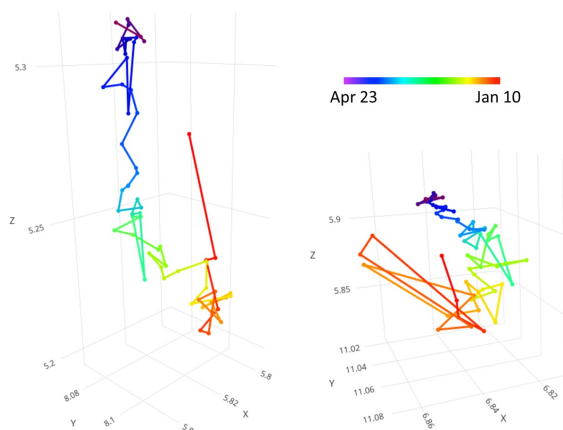


Figure 14. Trajectory of two distinctive branch points in 3D: point K (left) and point O (right).

The presented branch tracking algorithm reaches its limits because the branch points to be analysed are selected in the leafless reference epoch t_0 . Incorrect tracking may occur if the branch section is not sufficiently visible due to occlusion by growing leaves and the point cloud sections to be matched lie outside the spatial region (very large movement). This manifests itself in an incorrect ICP assignment, as with point M in Figure 13. These errors can be excluded by analysing the standard deviations of the ICP algorithm.

The indicated M3C2 distances and tracking differences are caused not only by leaf growth, but also by branch lowering due to the leaf weight (Fig. 15). External influences such as the tree's water balance (drought stress and precipitation) also have an effect.

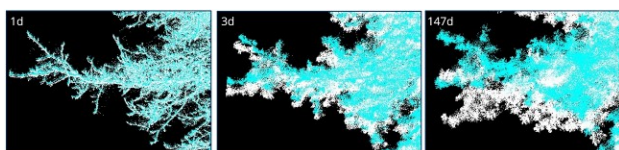


Figure 15. Exemplary representation of branch lowering over an observation period of one, three and 147 days. The turquoise point cloud represents the epoch recorded at an earlier time, while white represents the epoch recorded at a later time.

5. Conclusion and Outlook

The study investigated the potential of hyper-temporal TLS data for monitoring leaf growth and tree growth. The methods presented here show that a change in the crown can be detected by M3C2 distances. Two types of branch movement were detected: Annual movement of the branch and movement after rain events.

As the evaluation of the M3C2 distances showed, the branches lower after a rainfall event (within 24 hours). Within the next 24 hours, a lifting of the branches is visible, which is due to the elasticity of the wood and absorption of water. In addition to branch movements caused by precipitation, there are also annual branch movements. These are subject to a certain movement and can be described by tracking a defined point. The changes within the crown area are influenced by external influences (wind and rain), leaf emergence and growth and the general lowering of branches due to the gravity of the increasing leaf mass.

To answer the research outset questions: 1. Is it possible to detect leaf growth in the hyper-temporal recorded TLS data? Yes, it is possible to detect leaf growth in the data. In addition, heavy rainfall events affect the tree structure so that they are also visible in the data.

2. How does leaf growth and tree growth manifest itself in 3D tree parameters and point cloud comparisons? Leaf and tree growth can be identified in the data using the 3D tree parameters examined. While the DBH is a good indicator of stem growth, leaf growth can be recognized from the derived crown parameters (CPA and crown volume). The point cloud comparisons show little change after leaf emergence.

For further research questions regarding branch volume or occlusion modeling inside tree crowns based on time series, the movement behavior of branches is essential and requires consideration of the course of movement. Future work will focus on tracking and predicting these movements using applied Quantitative Structure Models (QSM). As the crown skeleton performs natural movements, these areas are severely constrained and cannot be predicted by rigid structural models.

Acknowledgement and funding

This work was supported by the German Research Foundation (Deutsche Forschungsgemeinschaft, DFG) [grant number 519022036]. We would also like to thank Ergo Umweltinstitut GmbH (data producer), Pikobytes GmbH (data distributor) and the Leibniz Institute of Ecological Urban and Regional Development – IOER (data owner) for providing the meteorological data. Furthermore, we would like to thank our colleagues who supported us with ongoing data collection throughout the year. Special thanks go to Prof. Roloff (Chair of Botany, Dresden University of Technology), who provided us with valuable information on tree biology.

References

Besl, P. J., McKay, N.D., 1992. A Method for Registration of 3-D Shapes. *IEEE Transactions on Pattern Analysis and Machine Intelligence*. 14 (2), 239–256. doi:10.1109/34.121791.

Bienert, A., Georgi, L., Kunz, M., von Oheimb, G., Maas, H.-G., 2021. Automatic extraction and measurement of individual

trees from mobile laser scanning point clouds of forests. *Ann. Bot.*, 128, 6, 787-804, <https://doi.org/10.1093/aob/mcab087>.

Campos, M. B., Litkey, P., Wang, Y., Chen, Y., Hyyti, H., Hyyppä, J., Puttonen, E., 2021. A Long-Term Terrestrial Laser Scanning Measurement Station to Continuously Monitor Structural and Phenological Dynamics of Boreal Forest Canopy. *Front. Plant. Sci.*, 11, 2132.

Dupuis J., Holst C., Kuhlmann H., 2017. Measuring Leaf Thickness with 3D Close-Up Laser Scanners: Possible or Not? *Journal of Imaging*, 3(2), 22.

Hallmark, A.J., Maurer, G.E., Pangle, R.E., Litvak, M.E., 2021. Watching plants' dance: Movements of live and dead branches linked to atmospheric water demand. *Ecosphere*, 12, e03705.

Hosoi, F., Nakabayashi, K., Omasa, K., 2011. 3-D modeling of tomato canopies using a high-resolution portable scanning lidar for extracting structural information. *Sensors*, 11(2), 2166-2174.

Junttila, S., Campos, M., Hölttä, T., Lindfors, L., Issaoui, A. E., Vastaranta, M., Hyyppä, H., Puttonen, E., 2022. Tree Water Status Affects Tree Branch Position. *Forests*, 13(5), Article 728. <https://doi.org/10.3390/f13050728>

Lague, D., Brodu, N., Leroux, J., 2013. Accurate 3D comparison of complex topography with terrestrial laser scanner: Application to the Rangitikei canyon (N-Z). *ISPRS Journal of Photogrammetry and Remote Sensing*, 82, 10-26.

Maas, H.-G., Bienert, A., Scheller, S., Keane, E., 2008. Automatic forest inventory parameter determination from terrestrial laserscanner data. *Int. J. Remote Sens.*, 29(5), 1579-1593.

Olivier, M.-D., Schneider, R., Fournier, R. A., 2017. A method to quantify canopy changes using multi-temporal terrestrial LiDAR data: Tree response to surrounding gaps. *Agric. For. Meteorol.*, 237, 184-195.

Puttonen, E., Briese, C., Mandlbürger, G., Wieser, M., Pfennigbauer, M., Zlinszky, A., Pfeifer, N., 2016. Quantification of overnight movement of birch (*Betula pendula*) branches and foliage with short interval terrestrial laser scanning. *Front. Plant. Sci.*, 7, 222.

Puttonen, E., Lehtomäki, M., Litkey, P., Näsi, R., Feng, Z., Liang, X., Wittke, S., Pandžić, M., Hakala, T., Karjalainen, M., Pfeifer, N., 2019. A clustering framework for monitoring circadian rhythm in structural dynamics in plants from terrestrial laser scanning time series. *Front. Plant. Sci.*, 10, 486.

Vitasse, Y., Baumgarten, F., Zohner, C.M., Rutishauser, T., Pietragalla, B., Gehrig, R., Dai, J., Wang, H., Aono, Y., Sparks, T.H., 2022. The great acceleration of plant phenological shifts. *Nat. Clim. Chang.*, 12, 300-302.

Zlinszky, A., Molnár, B., Barfod, A.S., 2017. Not All Trees Sleep the Same - High Temporal Resolution Terrestrial Laser Scanning Shows Differences in Nocturnal Plant Movement. *Front. Plant Sci.*, 8, 1814.